SECURITY INFORMATION

[redacted]

Copy 230
RM L51I14

[redacted]

NACA RM L51I14

TECH LIBRARY KAFB, NM
0143821

NACA

RESEARCH MEMORANDUM

7293

FREE-FLIGHT INVESTIGATION TO DETERMINE FORCE AND HINGE-MOMENT CHARACTERISTICS AT ZERO ANGLE OF ATTACK OF A 60° SWEPTBACK HALF-DELTA TIP CONTROL ON A 60° SWEPTBACK DELTA WING AT MACH NUMBERS BETWEEN 0.68 AND 1.44

By C. William Martz, James D. Church, and John W. Goslee

Langley Aeronautical Laboratory
Langley Field, Va.

CLASSIFIED DOCUMENT

[redacted]

NATIONAL ADVISORY COMMITTEE
FOR AERONAUTICS

WASHINGTON
December 3, 1951

[redacted]

S/9 98/13

Classification cancelled (or changed to UNCLASSIFIED)

By authority of NASA Tech Pub Announcement #107
(OFFICER AUTHORIZED TO CHANGE)

By ..... 9 Oct 56
NAME AND

RAD
GRADE OF OFFICER MAKING CHANGE)

4 Apr 61
DATE

TECH LIBRARY KAFB, NM
0143821

NATIONAL ADVISORY COMMITTEE FOR AERONAUTICS

RESEARCH MEMORANDUM

FREE-FLIGHT INVESTIGATION TO DETERMINE FORCE AND HINGE-MOMENT CHARACTERISTICS AT ZERO ANGLE OF ATTACK OF A 60° SWEPTBACK HALF-DELTA TIP CONTROL ON A 60° SWEPTBACK DELTA WING AT MACH NUMBERS BETWEEN 0.68 AND 1.44

By C. William Martz, James D. Church, and John W. Goslee

SUMMARY

A free-flight investigation of two rocket-powered control research models has been conducted to determine the force and hinge-moment characteristics, at zero angle of attack, of a half-delta tip control on a delta wing. Each of the models consisted of a cylindrical body, with ogival nose and tail sections, equipped with a cruciform arrangement of 60° sweptback delta wings, the wing panels in one plane being equipped with half-delta tip controls.

Data, obtained at zero angle of attack, are presented at various Mach numbers as the variation with control deflection of control normal-force coefficient, control normal-force chordwise center-of-pressure location, and control hinge-moment coefficient for various hinge-line locations.

Results show the half-delta tip control could be so hinged that very small hinge-moment coefficients due to control deflection would be obtained over the Mach number range from 0.68 to 1.44. Abrupt changes in control normal-force coefficient, chordwise center-of-pressure location, and hinge-moment coefficient occurred between the Mach numbers of 0.9 and 0.95. The control center-of-pressure location at small deflections was found to be fairly constant at 58 to 59.5 percent control root chord for subsonic speeds and at 65 to 66 percent root chord for supersonic speeds. Control normal-force coefficients were from 5 to 15 percent less than lift coefficients calculated by linear theory.

[redacted] PERMANENT RECORD

INTRODUCTION

In continuation of a program designed to determine force and moment characteristics of various control-surface configurations (reference 1), a 60° sweptback delta wing with half-delta tip controls was tested in free flight through the use of rocket-powered models. This wing-control configuration was chosen because of its good rolling-effectiveness characteristics (reference 2) and because the hinge line of the control could easily be located to provide good aerodynamic-balance characteristics.

Control hinge moments were obtained for several hinge-line locations from 58 to 68 percent of the control root chord at zero angle of attack for a range of control deflections of ±10° at Mach numbers from 0.68 to 1.44. These moment data were used to determine the magnitude and chordwise location of the control normal force. The results are presented herein and compared with results for a plain flap-type control surface and with linear theory.

SYMBOLS

b	wing span, 2.58 feet
$\bar{c}$	wing mean aerodynamic chord, 1.49 feet
$\bar{c}_a$	control mean aerodynamic chord, 4.62 inches
c_a	control root chord, 0.577 foot
S	total wing area in one plane, 2.89 square feet
S_a	area of one control surface, 0.0961 square foot
δ	deflection of one control surface, degrees
M	Mach number
ρ	mass density of air, slugs per cubic foot
V	free-stream velocity, feet per second
q	dynamic pressure, pounds per square foot $\left(\frac{\rho V^2}{2}\right)$
μ	air-viscosity coefficient, slugs per foot-second

[redacted]

R Reynolds number $\left(\frac{\rho \bar{c} V}{\mu}\right)$

g acceleration of gravity, 32.2 feet per second squared

H control hinge moment about hinge line, inch-pounds

C_h control hinge-moment coefficient $\left(\frac{H}{qS_a\bar{c}_a}\right)$

C_{N_a} control normal-force coefficient $\left(\frac{\text{Normal force on control surface}}{qS_a}\right)$

$\left(C_{N_\delta}\right)_F$ value of $\frac{\partial C_{N_a}}{\partial \delta}$ faired between $\delta = \pm 2^\circ$, per degree

c.p. center of pressure measured from control apex

C_{l_δ} $\frac{\partial\left(\frac{\text{Total aileron rolling moment}}{qbS}\right)}{\partial \delta}$, per degree (where δ is the average deflection of both controls used as ailerons)

MODELS

The research vehicles (models A and B) used in this investigation consisted of a cylindrical body, with ogival nose and tail sections, equipped with a cruciform arrangement of 60° sweptback delta wings. Model B also included a canard section incorporating a cruciform arrangement of nonmovable 60° sweptback delta canard fins. A drawing of the models showing over-all dimensions is presented in figure 1 and photographs of the models are shown in figure 2.

The following information applies to both models unless otherwise specified. The wings in one plane were equipped with 60° sweptback half-delta tip controls. The ratio of total control area to total exposed wing area in one plane (including control area) was 1/9. The wing panels had a modified hexagonal airfoil section, the maximum thickness ratio of which varied from 2.32 percent at the root chord (fuselage center line) to 8.93 percent at the parting line of the wing and tip control. The tip controls, fastened to the outboard ends of torque rods, had modified double-wedge airfoil sections with a constant ratio of thickness to chord

of 3 percent. These controls were machined from solid steel. The parting-line gap was 0.045 inch. Figure 3 is a sketch showing the detail dimensions of the wing and tip control, and figure 4 is a photograph of the wing-control assembly (model B).

The nonmovable canard fins of model B, shown in detail in figure 5, were $\frac{1}{3}$-scale reproductions of the exposed wings which were not equipped with controls.

INSTRUMENTATION

Each of the models was equipped with an NACA telemeter which transmitted the following flight data: normal acceleration, static and total pressure, deflection angle and hinge moments of each of two tip controls, and angular rolling velocity.

A control-position indicator and balances to measure control hinge moments were constructed as integral parts of a power unit which was mounted in the rear part of the wing section of each model.

In addition to this model instrumentation, radiosondes recorded atmospheric data at all flight altitudes shortly after the firings. Flight-path data were obtained with a radar tracking unit and C W Doppler radar was used to determine initial flight velocities. Photographic tracking was also employed to obtain visual records of the flights.

TECHNIQUE

The technique utilized in the investigation consisted of mechanically pulsing the controls as ailerons throughout the flight so that their deflection varied sinusoidally with time. The pulsing frequency was approximately four cycles per second and the amplitude $\pm 10^{\circ}$. This technique allowed the continuous measurement of hinge moments on each of the controls for all control deflections over the entire Mach number range of the tests.

From separate measurements of the hinge moments about each of the hinge-line locations and a knowledge of the chordwise locations of the hinge lines, the location and magnitude of the control normal force was determined as shown in the appendix. All hinge-moment data were corrected for inertia effects of the control and control linkage caused by the pulsing motion as well as the load deflection effects of the control linkage.

The response of the models to the sinusoidal control input involved motion about the roll axis only (substantiated by a normal accelerometer reading of approximately zero obtained at all Mach numbers presented). Thus, angle-of-attack effects upon the results were considered negligible except for the effect of the roll-induced helix angle at the control, which is subsequently discussed in the section on "Results and Discussion."

ACCURACY

All control normal-force data presented in the report were determined from hinge-moment measurements (see appendix). These measurements were obtained directly from telemetered deflections of calibrated moment beams. The small random errors which existed are best indicated by test point scatter.

Apart from the accuracy of the measurements is the "repeatability" factor which is an over-all indication of the percentage difference of comparable results obtained with two or more similar models. It is estimated that the repeatability factor for the present test is a maximum of approximately ±10 percent for the force and moment coefficients, whereas the chordwise location of the control normal force would be reproduced within ±2 percent of the control root chord.

RESULTS AND DISCUSSION

The variation of Reynolds number with Mach number is presented in figure 6 for models A and B.

All data presented in the report were obtained during decelerated flight (from 0 to -3.5 g) and at zero angle of attack. As shown in figure 6, model A results extended from subsonic to supersonic speeds while model B results were obtained only in the subsonic and transonic speed ranges. Although these test models differed in length and model B was equipped with fixed canard fins, the control moment data of these models were combined in the analysis of the data, since the spanwise location of the canard fins, being considerably inboard of the tip controls, would minimize any wake effects of the canards on the controls. Also, the downwash effects of the canard fins on the controls were believed to be very small because of the small value (0.4°) of the roll-induced helix angle at the canard tips.

CONTROL HINGE MOMENTS

As previously stated, hinge moments were measured on four individual control surfaces - these controls differing only in that they were pivoted about different chordwise hinge-line locations. The locations are indicated in figure 3(b). Figure 7 presents the measured variation of these hinge moments (in coefficient form) with control deflection. Parts (a) and (b) of this figure represent data from model A flight between the Mach numbers of 0.675 and 1.435. Parts (c) and (d) present data from model B for Mach numbers between 0.695 and 1.054. These data of figure 7 are basic hinge-moment-coefficient data from which the inertia moments and inertia-load friction effects of the pulsing motion as well as the load deflection effects of the control linkage have been removed. At first glance, these curves appear to have a noticeable amount of test point scatter. A closer examination, however, shows that there are actually two sets of test points - one measured while the control was moving from negative to positive deflections and the other measured in the adjacent part of the cycle when the control was moving from positive to negative deflections. For the purpose of analysis of the hinge moment data, these "hysteresis" loops were faired to a single curve which bisected the two sets of data as seen in figure 7. This "hysteresis" effect has been attributed to a combination of roll-induced angle of attack and additional friction due to flight loads. In order to remove the roll-induced angle-of-attack effects, the curves of figure 7 would have to be faired through the data points obtained at zero rolling velocity. For this investigation, the roll response of the models was such that the rolling velocity was approximately zero at the maximum control deflections. Calculations indicate that the difference in the results as obtained from both curve-fairing methods is within the experimental accuracy of the investigation. The effects of additional friction, although not definitely known, are believed to be small because the controls were mounted in roller and needle bearings.

It should be pointed out that the direction of rotation of the "hysteresis loops" in figure 7 is clockwise in parts (a), (b), and (c) while in part (d) the rotation is counterclockwise. This observation in conjunction with other known factors indicates that the center of pressure of the roll-induced angle-of-attack load on the controls is between 57.95 and 64.08 percent control root chord. The control loads and moments due to this helix-angle effect were not determined because of their relatively small magnitudes.

A careful inspection of these hinge-moment data also shows some data disagreement at the beginning and ending of the recorded cycles (see part (c) of fig. 7 for $M = 0.901$). This disagreement is an effect of Mach number, which varied about 0.025 over the cycle, and was considered in the fairing of the curves.

For purposes of further analysis, the hinge-moment data were reduced to control-force data which are discussed in the following section.

CONTROL NORMAL FORCE

The variation of control normal-force coefficient and chordwise center-of-pressure location with control deflection is presented in figures 8 and 9 for various Mach numbers between 0.70 and 1.435. The data of figure 8 were determined from a least squares analysis of the faired hinge-moment measurements (from fig. 7) of both models as explained in the appendix. The data of figure 9 were determined from the faired hinge-moment measurements (from fig. 7) of model A only (see appendix). The variation of control normal-force coefficient with control deflection is seen to be fairly linear for all Mach numbers presented. The dashed portions of the curves of figure 8 represent values that were determined in the region of higher positive deflections where the hinge-moment data of one of the hinge lines were incomplete. These moment values were approximated and combined with data from the other three hinge lines to yield the values presented.

Equally as important as the magnitude of the normal force in the determination of hinge moments is the chordwise location of the normal force. This information, presented in figures 8 and 9 as a function of control deflection, shows the center-of-pressure (c.p.) location at subsonic speeds to be approximately constant at 58 to 59.5 percent root chord for low deflections. As the deflection was changed to $\pm 8^{\circ}$ the center of pressure moved rearward from 1 to 2 percent root chord. At Mach numbers between 0.90 and 0.95, the center of pressure abruptly changed from the subsonic location to the low supersonic location of 64 to 65 percent root chord - the center of pressure moving rearward with increasing positive and negative deflections. At supersonic Mach numbers the center-of-pressure location was fairly constant with deflection at 65 to 66 percent root chord.

The effect of Mach number on the control normal-force data is shown in figure 10: part (a) presents the center-of-pressure data for a deflection near 0° and for a deflection of 8° and part (b) the slope of the normal-force coefficients at low deflections. Here, the solid curves represent values obtained from figure 8 which are the results of models A and B combined by the method of least squares. The curves labeled "Extrapolation based on model A results" were determined by shifting the results of model A (taken from fig. 9) along the ordinates of the curves of figure 10 so as to produce a continuous Mach number history of the variables at $M = 1.05$, the Mach number at which the two reduction methods overlapped. The magnitude of this shift was about 0.006 for the normal-force coefficient and 1/2 percent root chord for the

center-of-pressure data. Since the moment data of the four individual hinge lines tested were considered of equal accuracy, the results obtained by combining the data of both models (four hinge lines) should be more accurate from a statistical standpoint than those determined by model A alone (two hinge lines). Therefore, the shifting of the model A results along the ordinates in figure 10 to agree with the combined results of both models at $M = 1.05$ is believed justified. Shown for comparison in figure 10 are theoretical values of the control chordwise center of pressure and control lift-curve slope. These values were calculated for the tip control used in the present investigation through the use of linear theory (reference 3).

Figure 10(a) shows the experimental values of center of pressure to be in good agreement with linear theory which predicts a location of 2/3 root chord at supersonic Mach numbers. The principal effect of Mach number on the location of the center of pressure is seen to be the rather abrupt rearward shift between the Mach numbers of 0.9 and 0.95. At the larger deflections, this rearward shift is more gradual than for the smaller deflections. This fact helps explain the asymmetrical values of center of pressure presented in figure 8 for small deflections at $M = 0.90$. The suddenness with which the center of pressure changed location was of such a degree that the test data, recorded in cycles of 0.25-second duration, show a difference in center-of-pressure location within a portion of one cycle. The values of center-of-pressure location at the higher deflections, however, were more symmetrical because of the gradual shift as shown on figure 10(a). The nearly constant location of the center of pressure at subsonic speeds (58 to 59.5 percent root chord) and supersonic speeds (65 to 66 percent root chord) is readily noticed in a plot of this type.

The ability of linear theory to predict the normal-force-coefficient slope, $(C_{N\delta})_F$, is illustrated in figure 10(b). Here, theoretical values are from 5 to 15 percent larger than measured values. This result is to be expected because the effects of viscosity, gap at the wing control juncture, and airfoil thickness are not considered in the theory. In contrast to the nearly constant value of $(C_{N\delta})_F$ obtained at subsonic speeds, the value of $(C_{N\delta})_F$ increased abruptly at a Mach number of 0.9 to a maximum value of $(C_{N\delta})_F = 0.048$ at $M = 0.975$. This value is decreased 30 percent as Mach number increases from 0.975 to 1.435.

CALCULATED HINGE MOMENTS

As a means of illustrating the effects of various hinge-line locations on the hinge-moment deflection characteristics of the controls

reported herein, figure 11(a) was prepared from calculations involving the data of figures 8 and 9 and the physical characteristics of the control. Values of C_h/δ are presented as a function of Mach number for various hinge-line locations, the curves being based on a deflection of -5° and zero angle of attack. It should be noted that C_h/δ can be calculated similiarly for any chordwise hinge-line location and for any deflection up to $\pm 10^\circ$. The values of C_h/δ from the present test are seen to be very small over the large range of hinge-line locations and Mach numbers presented. Each of the curves for the different hinge lines are smooth over the Mach number range presented except between the Mach numbers of 0.90 and 0.95 where the values of C_h/δ abruptly increased in a negative direction. The effect of chordwise hinge-line location on C_h/δ is such that the value of C_h/δ is directly proportional to the chordwise distance between the hinge line and the control center of pressure. Shown for comparison, in figure 11(a), are values of C_h/δ for a hinge-line location of 63.50 percent control root chord as obtained from previous rocket test results (reference 1) for a configuration similar to model A of the present investigation. Although, the Mach number trend of these values compares very favorably with the trend of the present test results, the values of reference 1 are all displaced along the C_h/δ axis with respect to the present test results. This displacement is explained by the fact that the control surface used in reference 1 was constructed of duralumin, whereas the controls of the present test were of heat-treated steel. The duralumin control, being about 3 times as elastic as the steel controls, deflected more under flight loads. This load deflection was accompanied by a forward movement of the control center of pressure. The magnitude of the difference in movement between the centers of pressure of the 3-percent-thick dural and steel controls (3 to 4 percent control root chord) agrees very well with unpublished results of an independent static loading test of a similar control of 4-percent thickness where the difference in movement was calculated to be 2.64 percent control root chord at $M = 1.5$. From the foregoing, it is apparent that control flexibility should be considered in the design of thin controls where a high degree of aerodynamic balance is desired.

In an attempt to provide a better basis for comparison of different hinge-line locations, the C_h/δ values of the present test, figure 11(a), were multiplied by standard sea-level values of dynamic pressure. This resulted in values of $H/S_a \bar{C}_a \delta$ a hinge-moment parameter proportional to the physical characteristics of the control surface. These values are presented in figure 11(b) as a function of hinge-line location and Mach number. Again, the curves are based on a deflection of -5° and zero angle of attack. As in figure 11(a), positive values indicate the control is statically unstable. Conversely, negative values denote positive stability of the control.

When the requirements of any particular control system are known, the selection of an optimum hinge-line location is expedited with a plot of this type. If the use of an automatic control system with servo-control units is considered, the sense or direction of the control moments is not too important. The magnitude of the moment, however, is very important as it regulates the space and weight requirements of the servo system. For use with a servo system, therefore, figure 11(b) suggests a hinge-line location of 64 percent root chord to provide minimum control moments due to deflection over the Mach number range presented. If a human pilot without the use of a booster control system is considered, both the magnitude and direction of the control moments are important. The hinge-line location, chosen to meet these requirements by providing the adequate control stability in combination with minimum control moments, would be located at approximately 56 percent root chord. For this location, however, the large variation of control moments over the Mach range would be undesirable to the pilot. As an improvement to this situation, the method of spring loading the control system can be applied. Spring loading effectively introduces an artificial stability effect into the control system, the values of $H/S_a\bar{c}_a\delta$ being increased negatively an equal amount at all Mach numbers. Linear interpolation of the curves of figure 11(b) show that a curve for a hinge-line location of approximately 68 percent chord, if moved negatively an appropriate amount along the $H/\bar{c}_aS_a\delta$ scale, would allow positive control-system stability at all Mach numbers and a much reduced variation of control deflection moments over the Mach range.

In order to indicate the aerodynamic advantages of the wing-tip aileron as compared to a plain flap-type trailing-edge aileron, figure 12 was prepared. Values of $\frac{C_h/\delta}{C_{l_\delta}}$ (an effectiveness parameter proportional to hinge moment per unit roll control effectiveness) as calculated for the wing-control configuration of the present investigation and for the trailing-edge plain flap-type control of reference 4, (installed on a wing of similar plan form) are presented as a function of Mach number for a deflection of -5° at zero angle of attack. Results are shown for hinge-line locations of 60.00 percent c_a, 64.00 percent c_a, and 68.00 percent c_a for the wing-tip control. In general, a minimum magnitude of $\frac{C_h/\delta}{C_{l_\delta}}$ is most desirable for automatic roll stabilization and control. Throughout the Mach range tested, $\frac{C_h/\delta}{C_{l_\delta}}$ values of the wing-tip control for all hinge-line locations presented are seen to be small as compared to the plain flap-type trailing-edge control. As previously stated in the discussion, the center of pressure of the roll-induced angle-of-attack loads on the control was deduced (from the data

of figure 7) to be between 57.95 and 64.08 percent control root chord. The hinge-line location of 0.60 c_a in figure 12 was chosen, therefore, to illustrate the fact that the hinge line could be located very near the center of pressure of the roll-induced angle-of-attack loads (so as to minimize helix angle effects on control moments) and still exhibit small values of $\frac{C_h/\delta}{C_{l_\delta}}$.

It should be pointed out that the large supersonic values of $\frac{C_h/\delta}{C_{l_\delta}}$ for the trailing-edge flap resulted mainly from the large values of C_h/δ. These values could be substantially reduced by moving the hinge line rearward to provide aerodynamic balance. However, for airfoils less than 7 percent thick, the extremely thin sections at the wing trailing edge make it difficult to hinge the control rearward of its 30 percent chord.

CONCLUDING REMARKS

The following remarks have been concluded from the results of an investigation at zero angle of attack between the Mach numbers of 0.68 and 1.44 of a 60° sweptback half-delta tip control installed on a 60° sweptback delta wing:

1. Values of C_h/δ, as obtained for the range of Mach numbers tested and for various hinge-line locations, are comparatively small for the half-delta tip control.

2. The experimental normal-force values of the half-delta control were from 85 to 95 percent of theoretical lift values calculated by linearized theory. An abrupt increase in normal force of 26 percent occurred as Mach number was increased from 0.90 to 0.98. The variation of normal force with Mach number was gradual at all other speeds tested.

3. The chordwise location of the control center of lift at small deflections remained fairly constant at 58 to 59.5 percent root chord for Mach numbers up to 0.95 and at 65 to 66 percent root chord for supersonic Mach numbers. An abrupt rearward shift in location of the center of pressure, especially at low deflections, occurred between the Mach numbers of 0.90 and 0.95 where the center of pressure moved from the subsonic to the supersonic location. Between the Mach numbers of 0.8 and 0.95, the effect of deflection on center-of-pressure location was most pronounced (from 1 to $2\frac{1}{2}$-percent rearward shift for a deflection

increase of ±8°). At all other Mach numbers presented, the center-of-pressure location was changed about 1 percent root chord for the same deflection increase.

4. Results indicate the half-delta tip control can produce more rolling effectiveness per unit hinge moment than the plain flap-type control surface.

Langley Aeronautical Laboratory
National Advisory Committee for Aeronautics
Langley Field, Va.

APPENDIX

REDUCTION OF HINGE-MOMENT DATA TO OBTAIN MAGNITUDE AND CHORDWISE LOCATION OF CONTROL NORMAL-FORCE COEFFICIENT

As stated in the text of the report, hinge-moment data were obtained from each of four control surfaces. Figure 3(b) shows the hinge-line locations in percent root chord for each of the four controls tested. Since the controls were of identical construction, it was possible to assume the magnitude, direction, and location of the normal-force coefficient to be identical for the four controls when compared at the same longitudinal control deflection and Mach number. It should be noted here that this assumption is not entirely correct. Although one of the controls was located with respect to the wing so that the leading and trailing edges were in line with the leading and trailing edges of the wing (control 2), the other controls were slightly staggered with respect to a normal in-line location. It is believed that the effect of the staggered control projecting forward of the leading edge of the wing would be to relieve the load on that part of the control and move the center-of-pressure rearward. However, the magnitude of this load redistribution is believed to be very small for the present investigation and its effect on the results was considerably reduced by the least squares or curve-fitting method of analysis. It follows, therefore, that for equal deflections and Mach numbers, the hinge-moment coefficients of the four controls are directly proportional to the chordwise distances between their respective hinge-line locations and the control centers of pressure.

The following discussion applies between the Mach numbers of 0.695 and 1.054 where data were obtained from both models A and B. The data from figure 7 were plotted against Mach number for the various control deflections, so that hinge-moment coefficients for each of the four

controls at a given longitudinal control deflection and Mach number could be plotted against percent root chord as shown in the following figure:

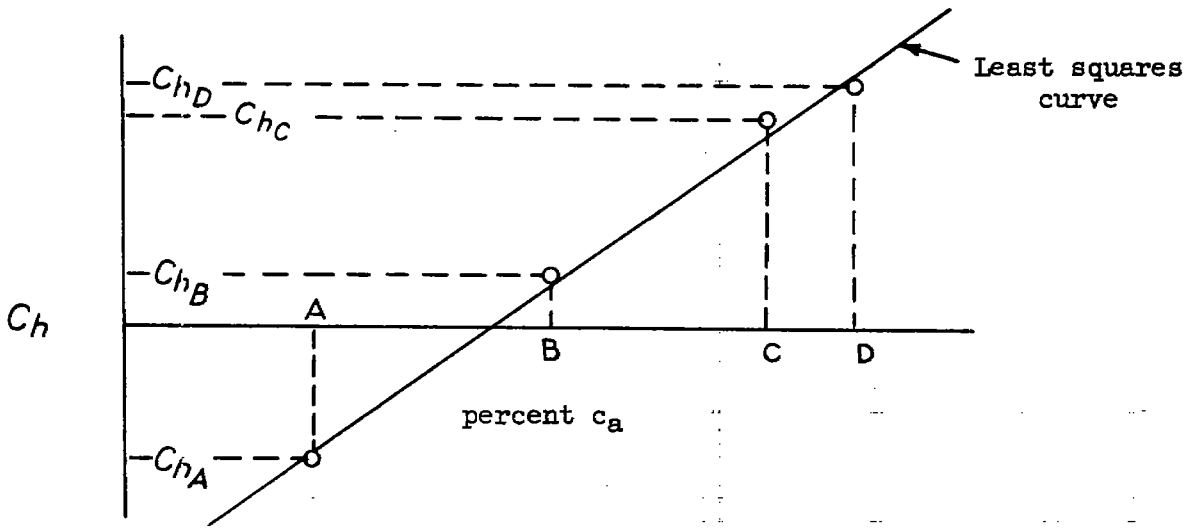

where A, B, C, and D are the chordwise hinge-line locations of the four controls, and C_{h_A}, C_{h_B}, C_{h_C}, and C_{h_D} are respective hinge-moment coefficients of the four controls at a given deflection and Mach number (determined from a cross plot of the data from figure 7 with out-of-trim values removed).

A straight-line curve was then faired between the data points through the use of least squares. The intersection of this curve with the $C_h = 0$ axis determined the chordwise location of the control center of pressure and the control normal-force coefficient was equal to two-thirds the slope of the faired curve.

Actually, in the analysis of the data the faired straight-line curve and its slope and intercept were determined mathematically - the foregoing figure being used only for a graphical explanation.

Between the Mach numbers of 1.05 and 1.435, the data of model A were used in the same manner to determine the control normal force and chordwise center of pressure shown in figure 9. However, as data for only two hinge-line locations were available in this instance, a least squares application was unnecessary - the results being determined mathematically by considering the straight-line curve to pass directly through the two test points.

REFERENCES

1. Martz, C. William, and Church, James D.: Flight Investigation at Subsonic, Transonic, and Supersonic Velocities of the Hinge-Moment Characteristics, Lateral-Control Effectiveness, and Wing Damping in Roll of a 60° Sweptback Delta Wing with Half-Delta Tip Ailerons. NACA RM L51G18, 1951.

2. Sandahl, Carl A., and Strass, H. Kurt: Comparative Tests of the Rolling Effectiveness of Constant-Chord, Full-Delta, and Half-Delta Ailerons on Delta Wings at Transonic and Supersonic Speeds. NACA RM L9J26, 1949.

3. Lagerstrom, P. A., and Graham, Martha E.: Linearized Theory of Supersonic Control Surfaces. Jour. Aero. Sci., vol. 16, no. 1, Jan. 1949, pp. 31-34.

4. Mitcham, Grady L., Stevens, Joseph E., and Norris, Harry P.: Aerodynamic Characteristics and Flying Qualities of a Tailless Triangular-Wing Airplane Configuration as Obtained from Flights of Rocket-Propelled Models at Transonic and Low Supersonic Speeds. NACA RM L9L07, 1950.

SECURITY [redacted]

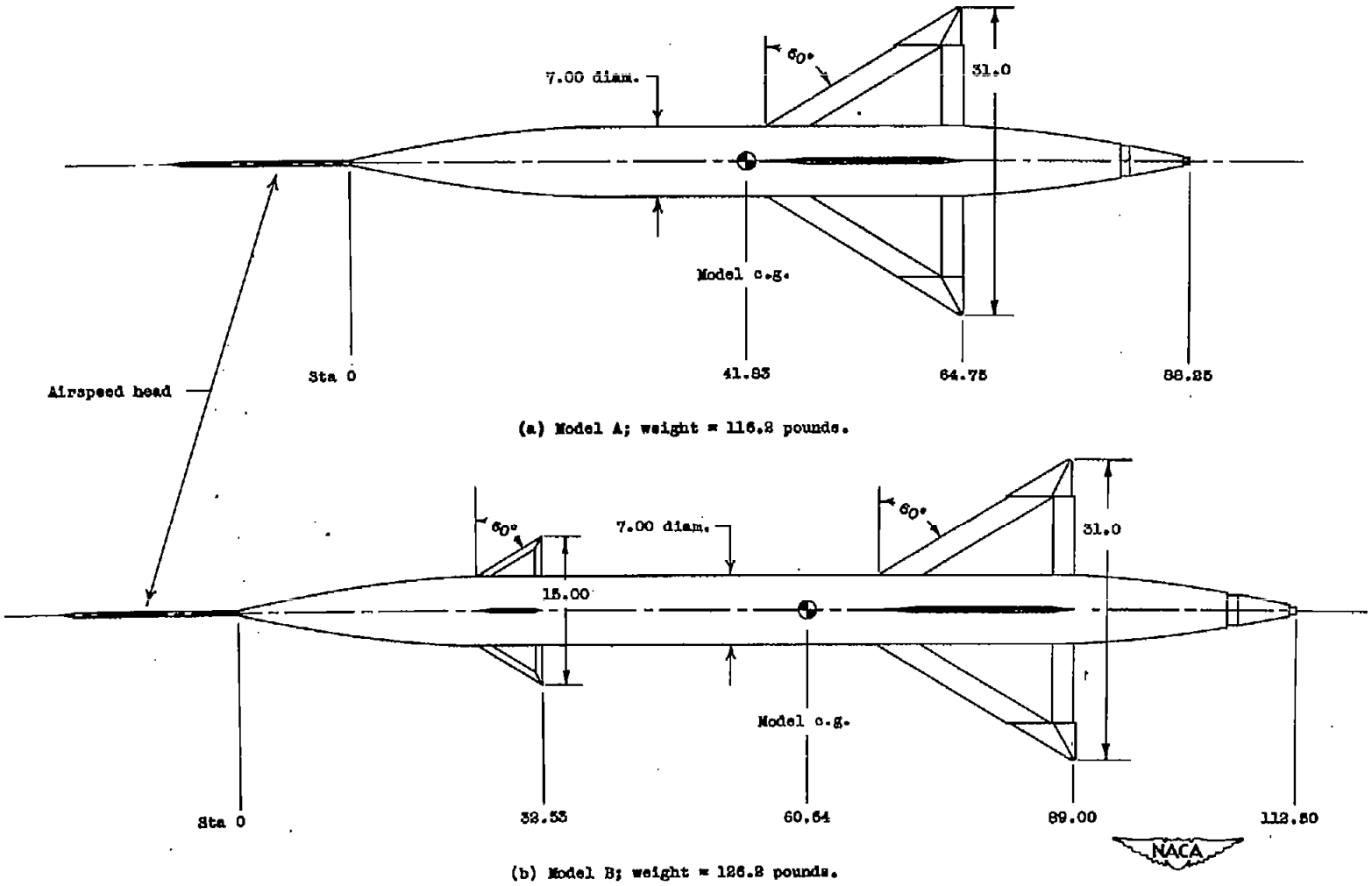

Figure 1.- General arrangement of test models. All dimensions in inches.

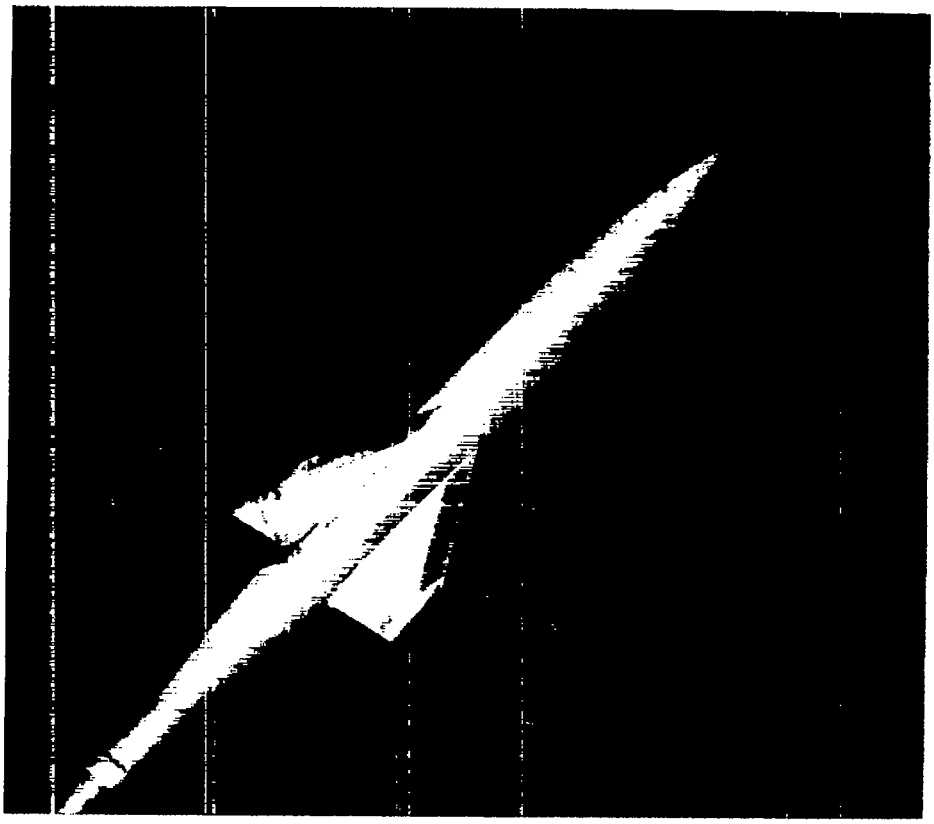

(a) Model A preparatory to flight. L-63733.1

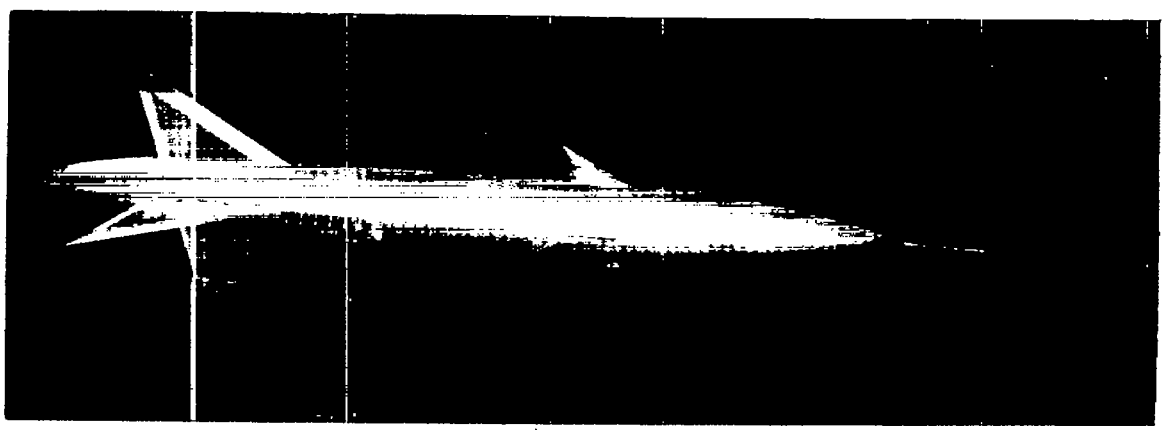

(b) Model B. L-65526.1

Figure 2.- Photographs of test models.

SECURITY INFORMATION

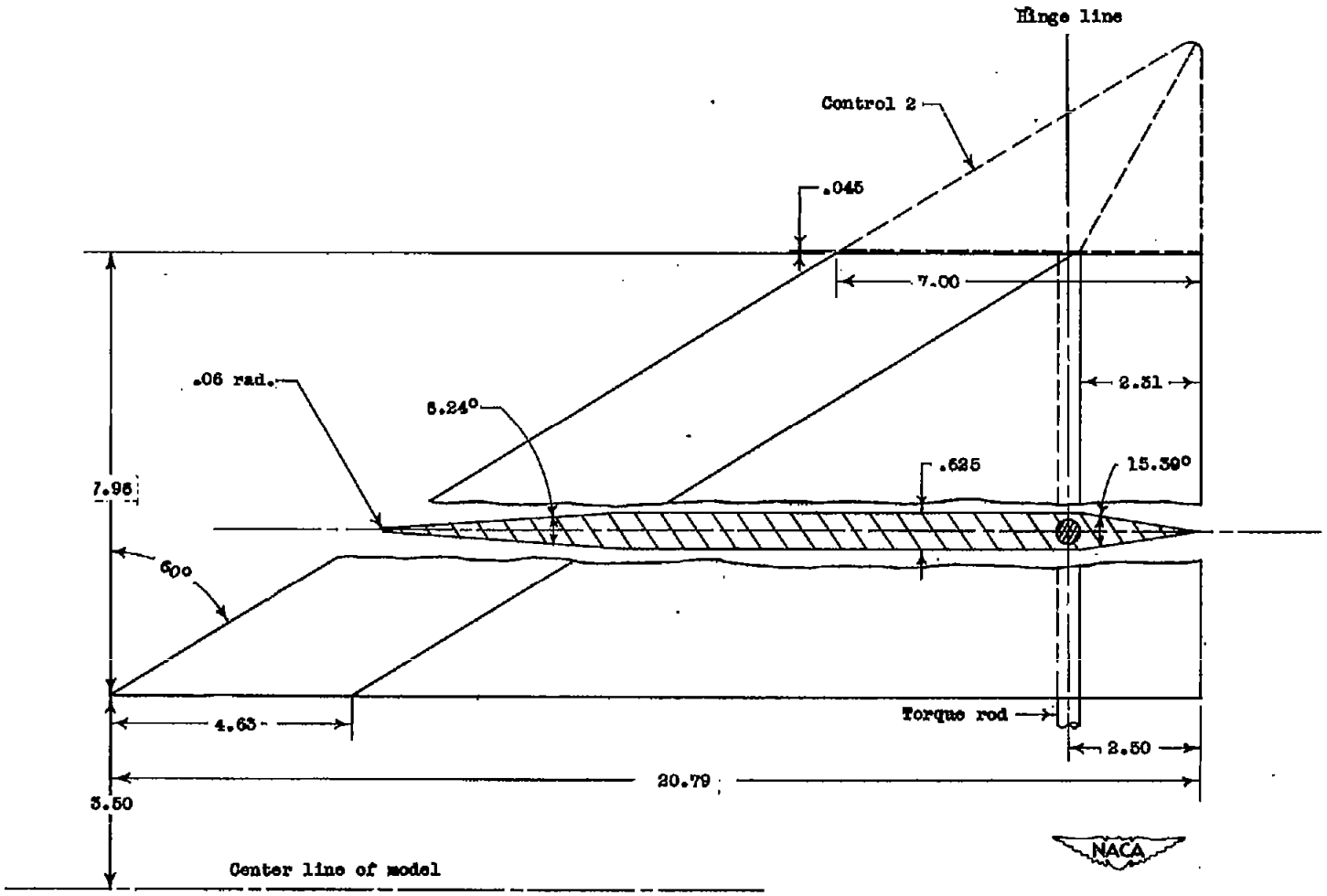

(a) Details of wing showing control 2 for reference.

Figure 3.- Control wing. All dimensions in inches.

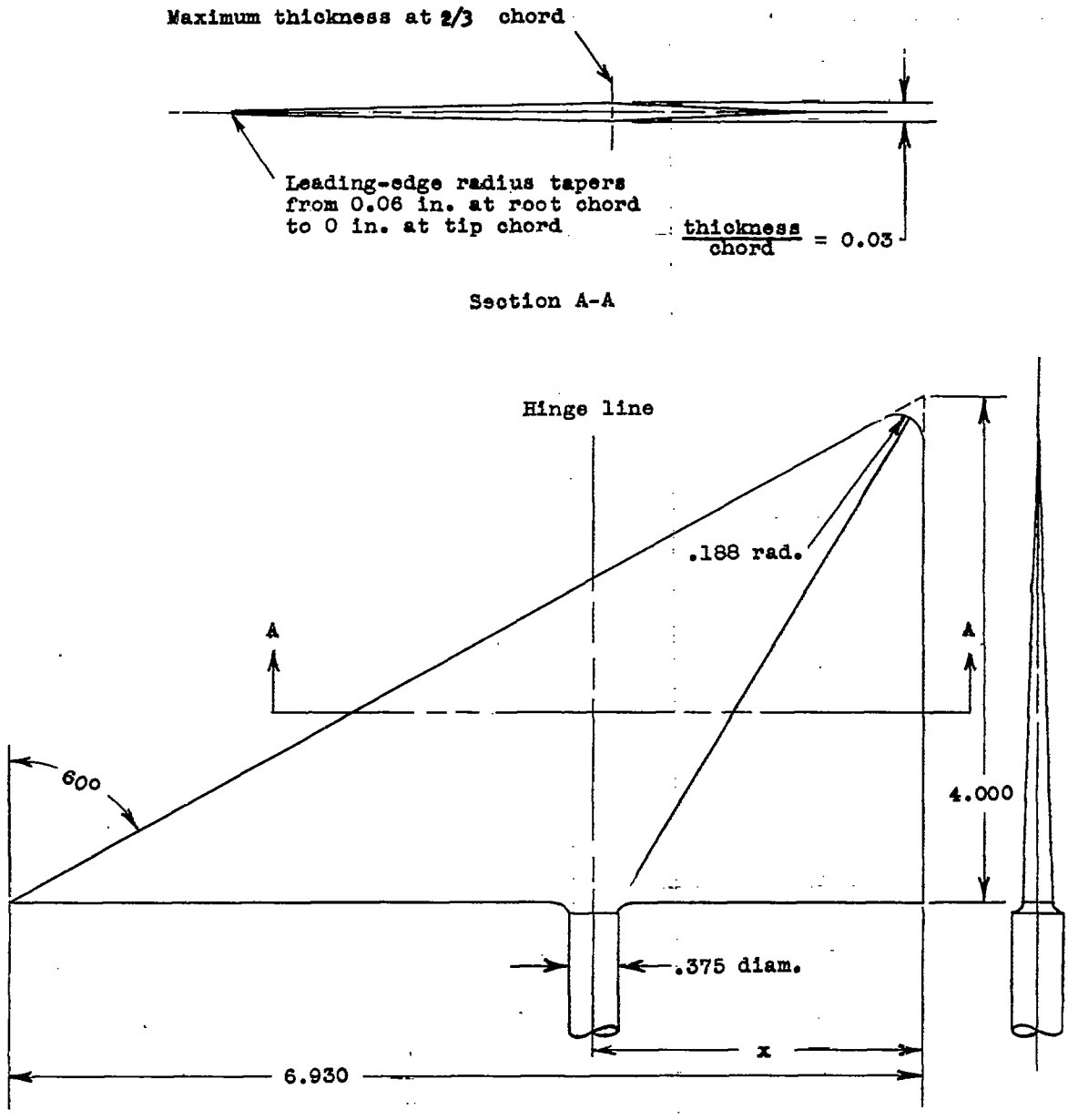

Model A	Control 1; $x = 2.238$ (Hinge line at $0.6770\ c_a$)
	Control 2; $x = 2.489$ (Hinge line at $0.6408\ c_a$)
Model B	Control 3; $x = 2.256$ (Hinge line at $0.6745\ c_a$)
	Control 4; $x = 2.914$ (Hinge line at $0.5795\ c_a$)

(b) Details of control.

Figure 3.- Concluded.

SE[redacted]

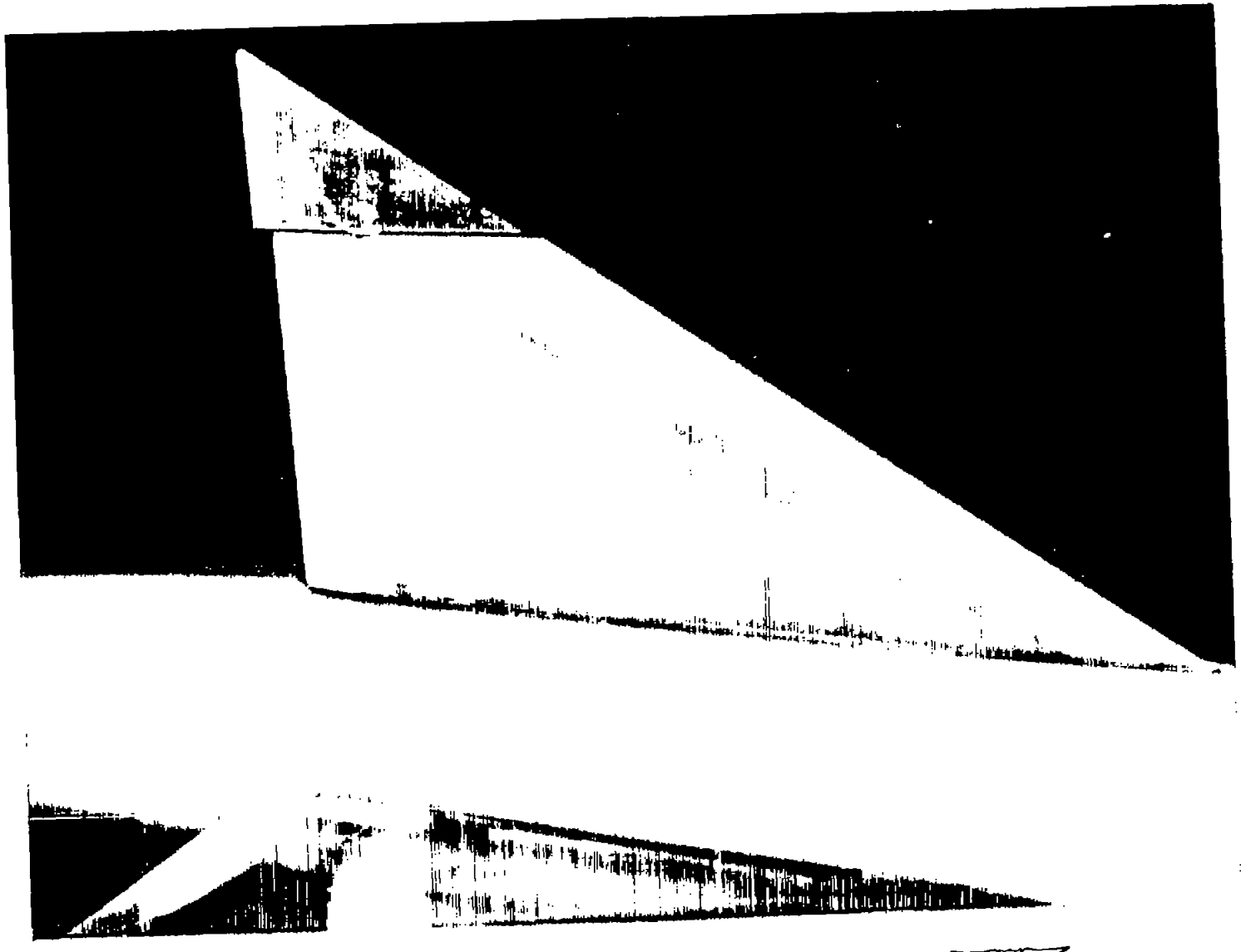

Figure 4.- Photograph of wing control assembly of model B. L-65528.1

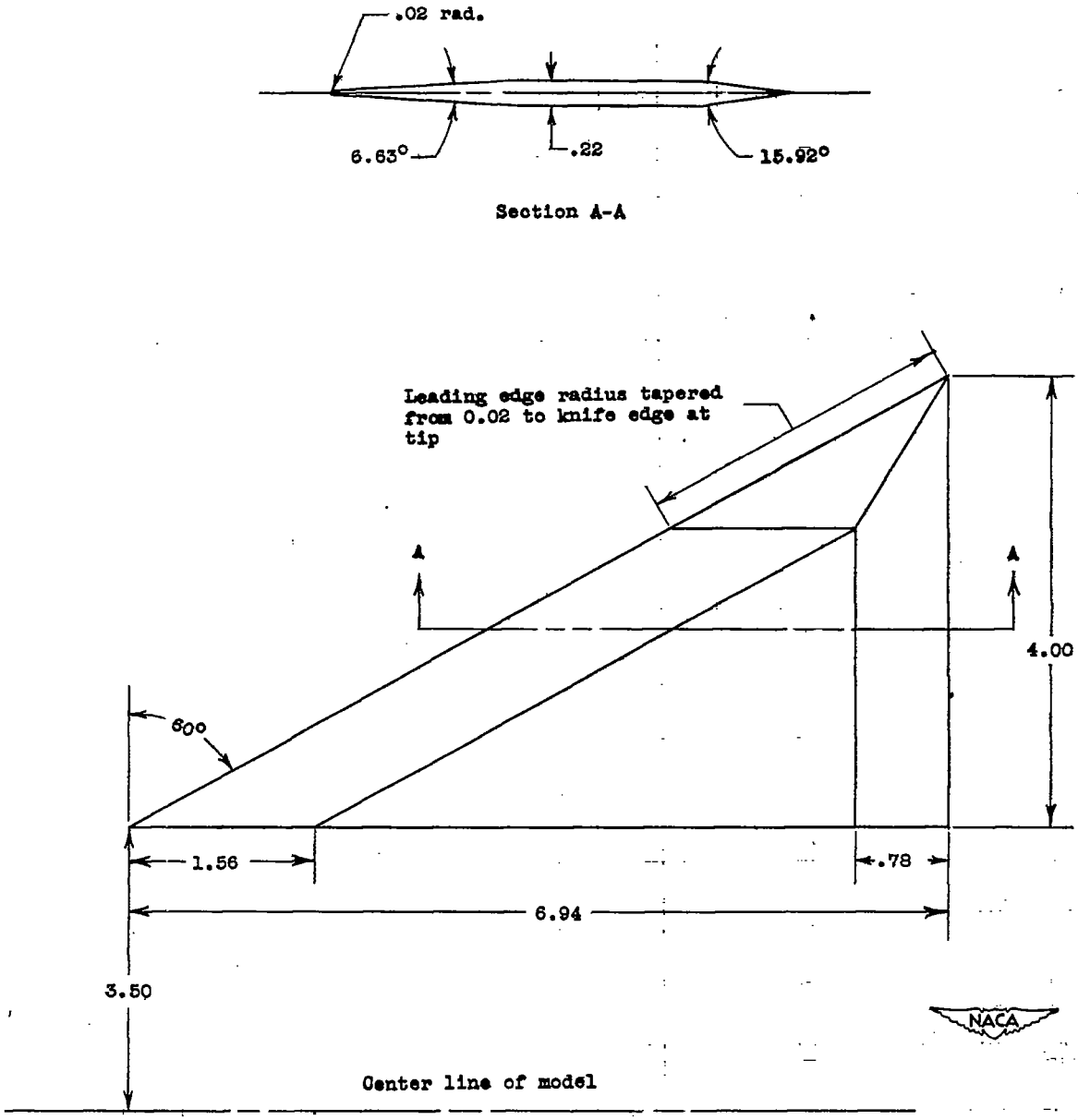

Figure 5.- Details of canard fins. All dimensions in inches.

SECURITY INFORMATION

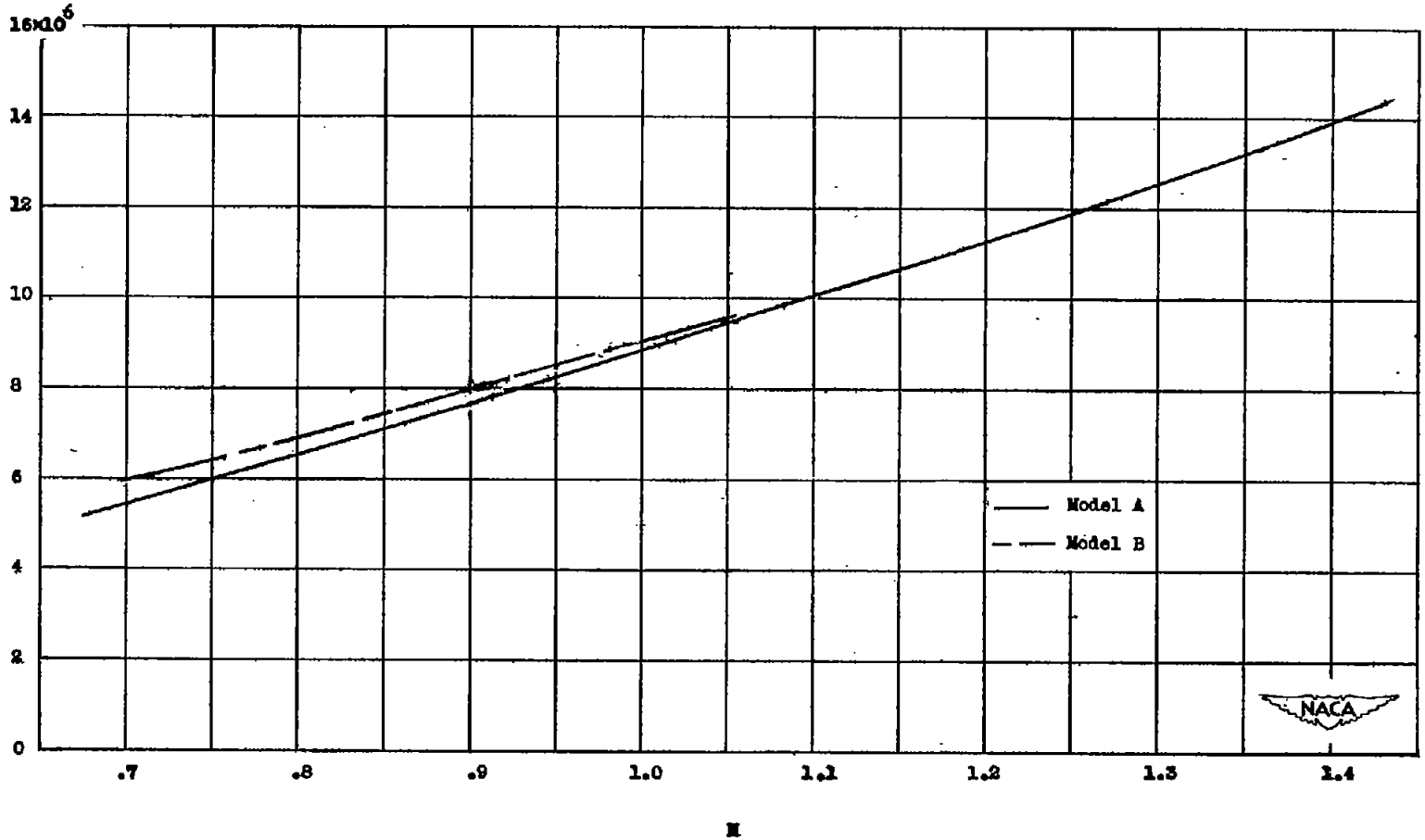

Figure 6.- Variation of Reynolds number with Mach number. Reynolds number is based on wing mean aerodynamic chord.

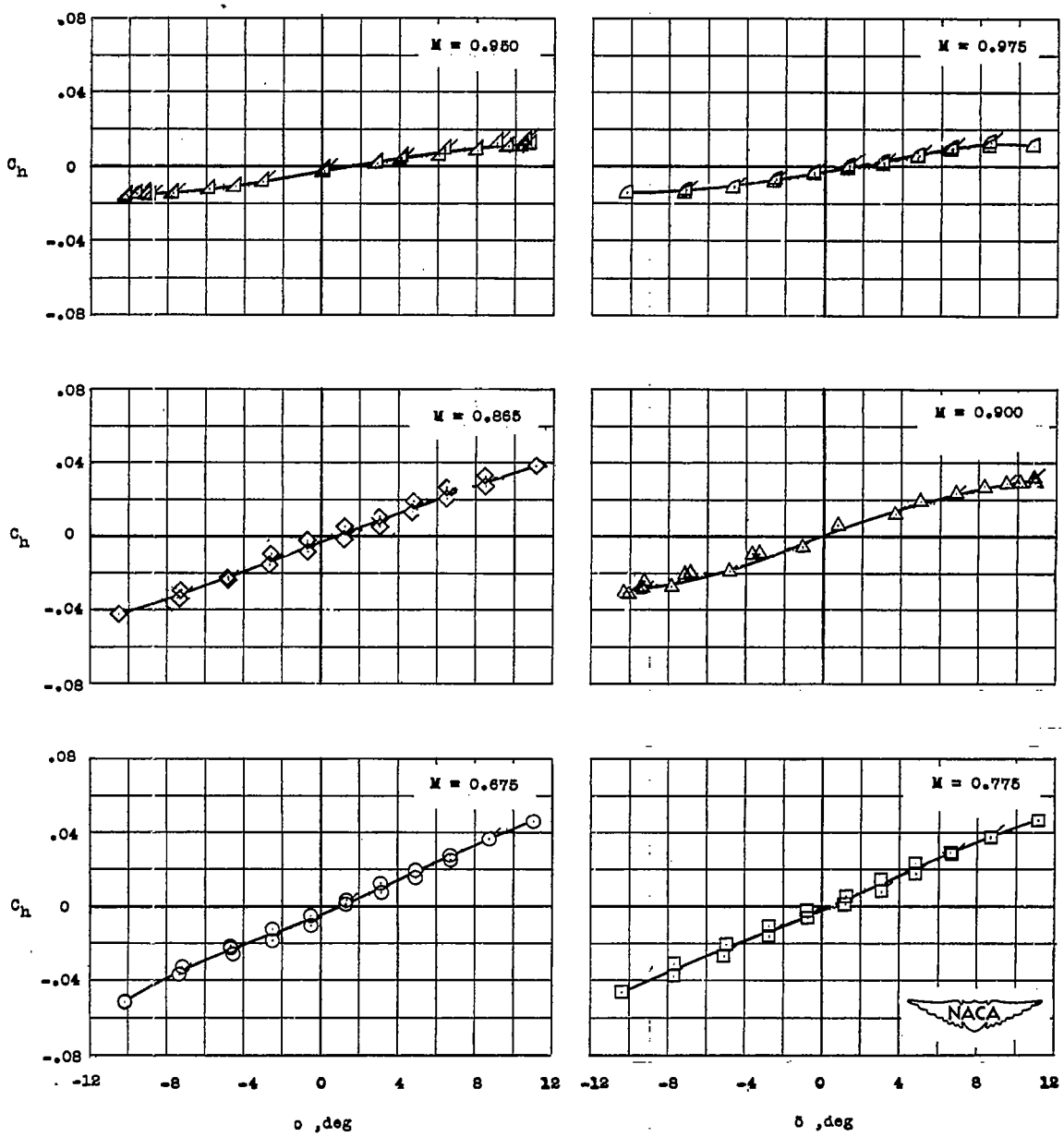

(a) Hinge line at $0.6770c_a$; model A.

Figure 7.- Control hinge-moment coefficient of models A and B plotted against control deflection for $M = 0.675$ to $M = 1.435$; $\alpha = 0^{\circ}$. Unflagged symbols represent movement of δ in a positive direction (from minus to plus) and flagged symbols show motion of δ in a negative direction.

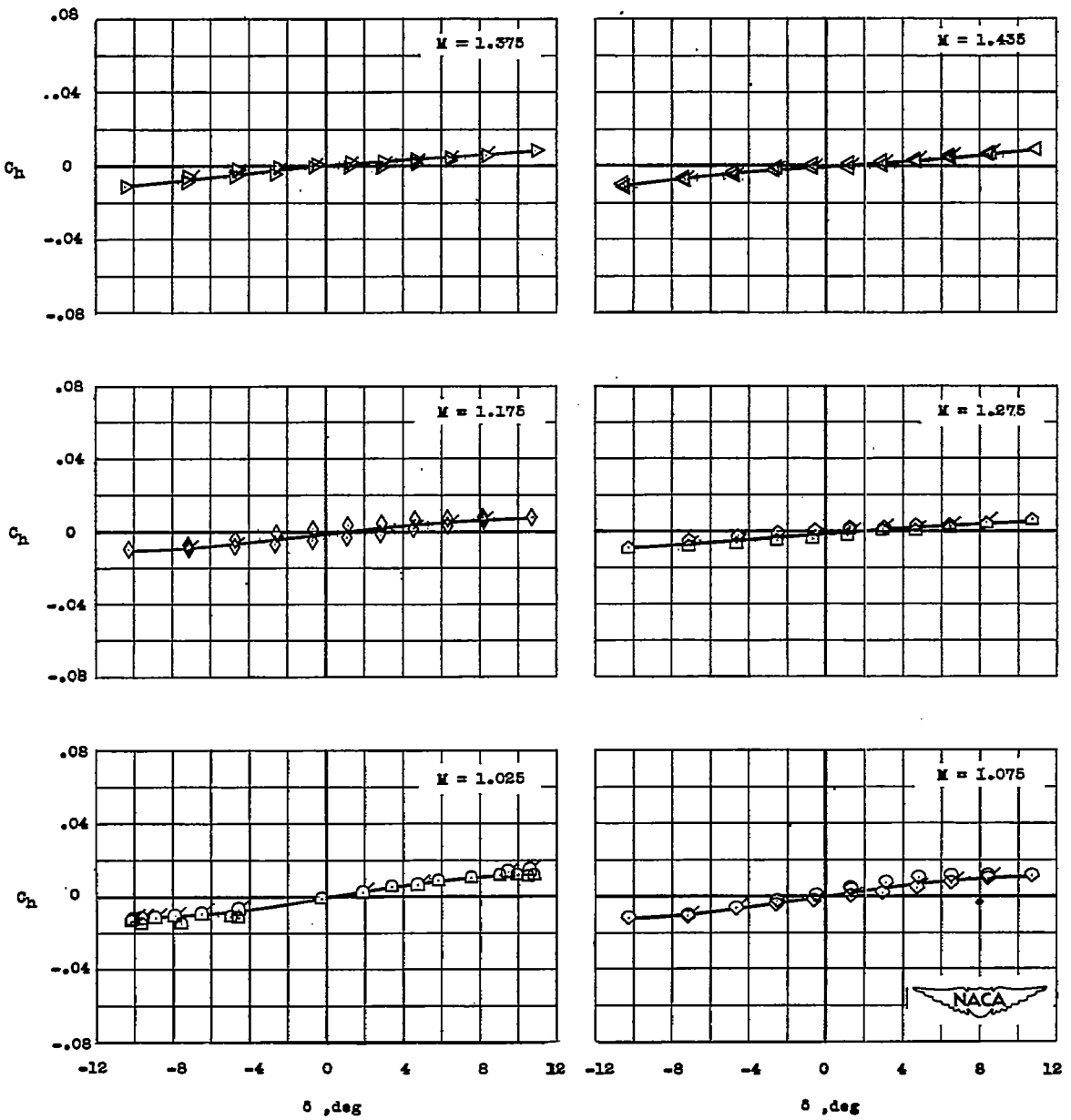

(a) Concluded.

Figure 7.- Continued.

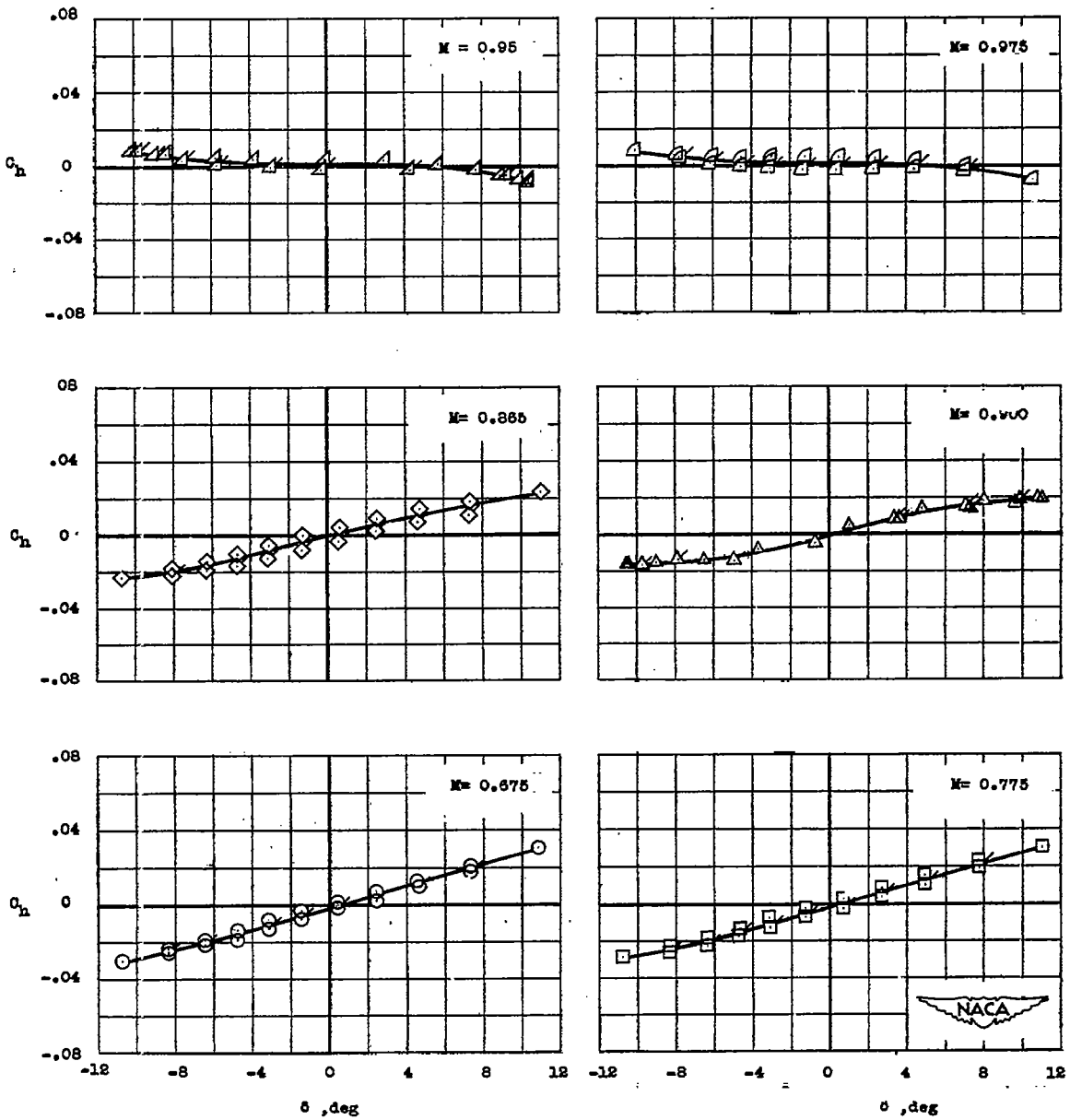

(b) Hinge line at $0.6408c_a$; model A.

Figure 7.- Continued.

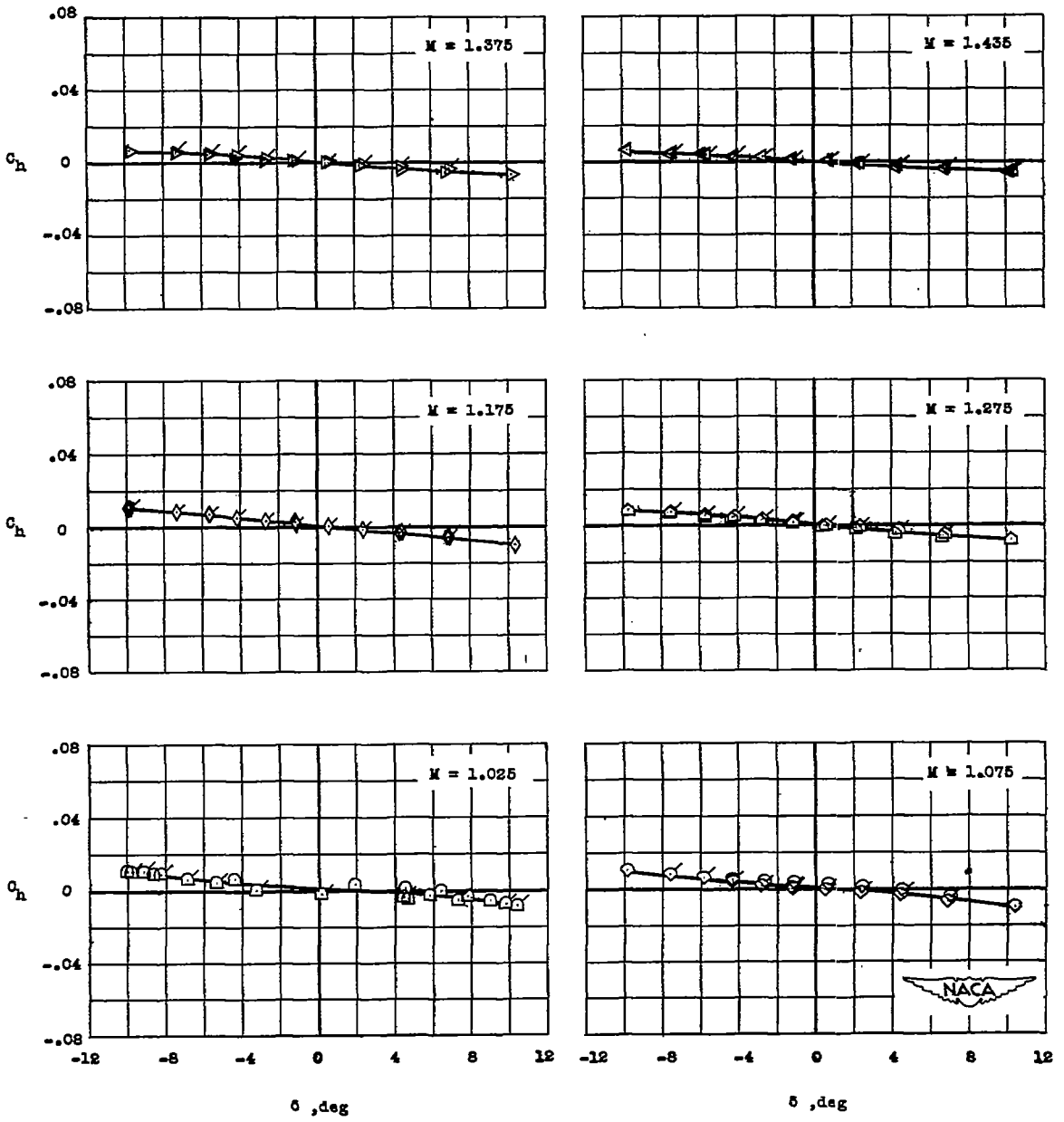

(b) Concluded.

Figure 7.- Continued.

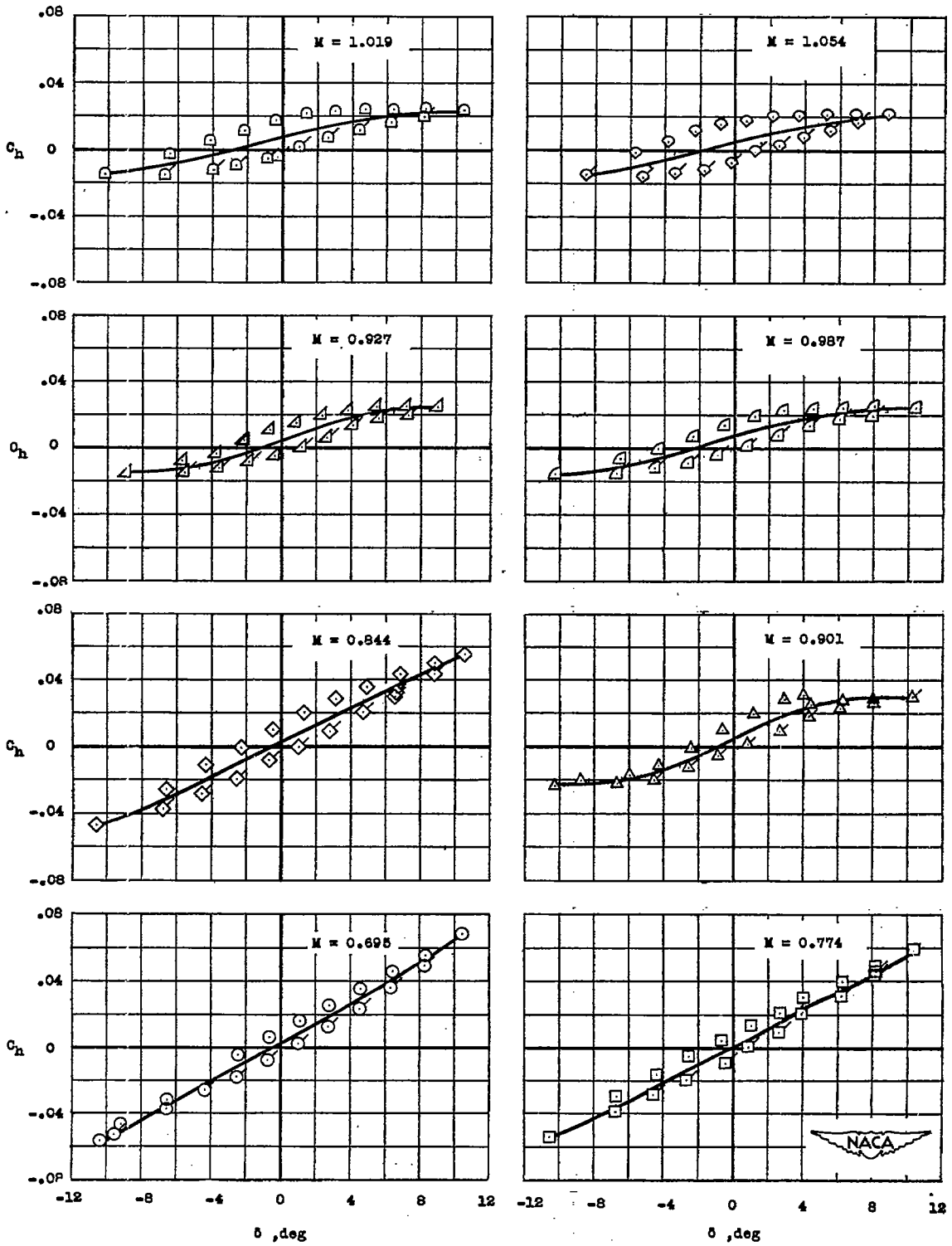

(c) Hinge line at $0.6745c_a$; model B.

Figure 7.- Continued.

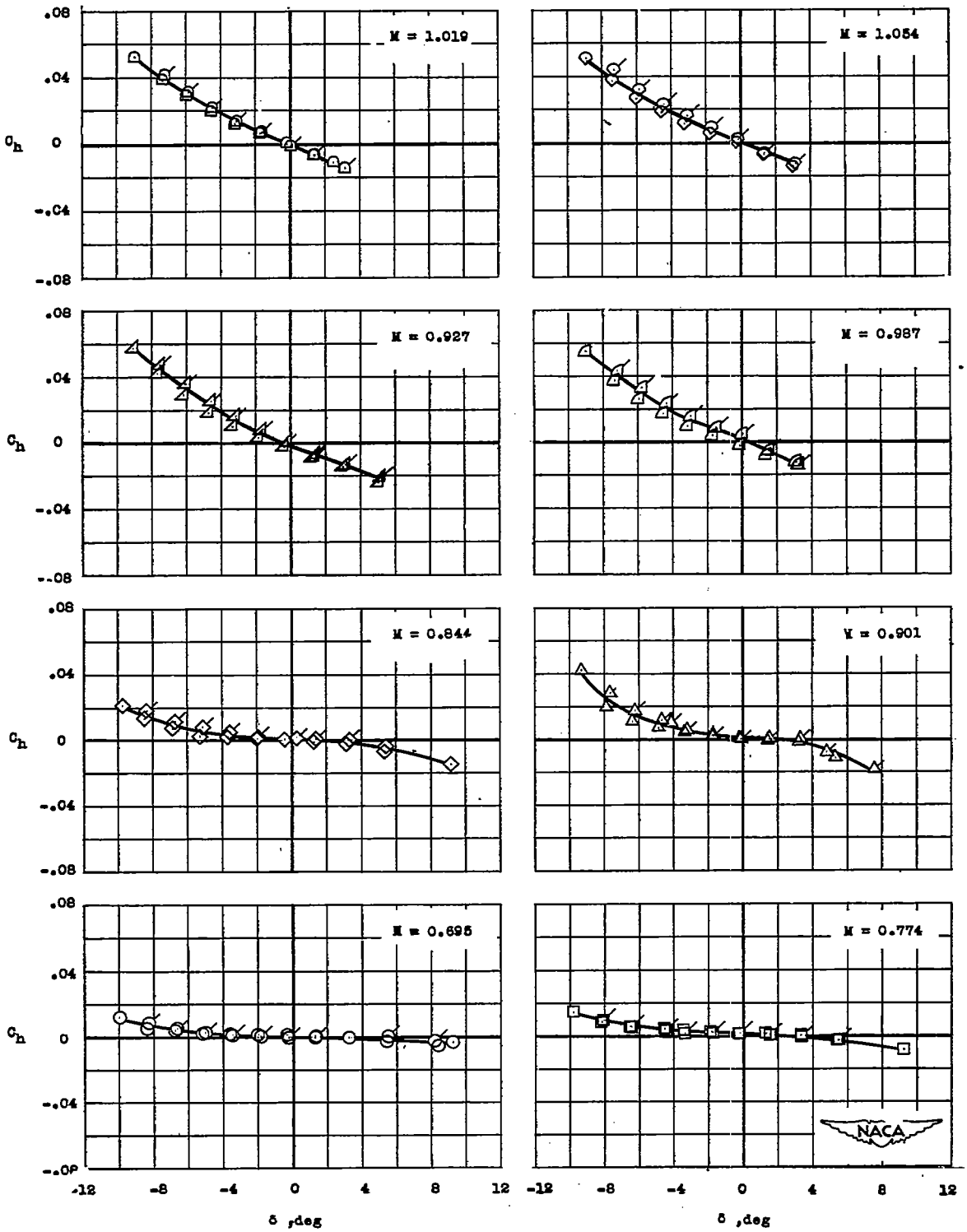

(d) Hinge line at $0.5795c_a$; model B.

Figure 7.- Concluded.

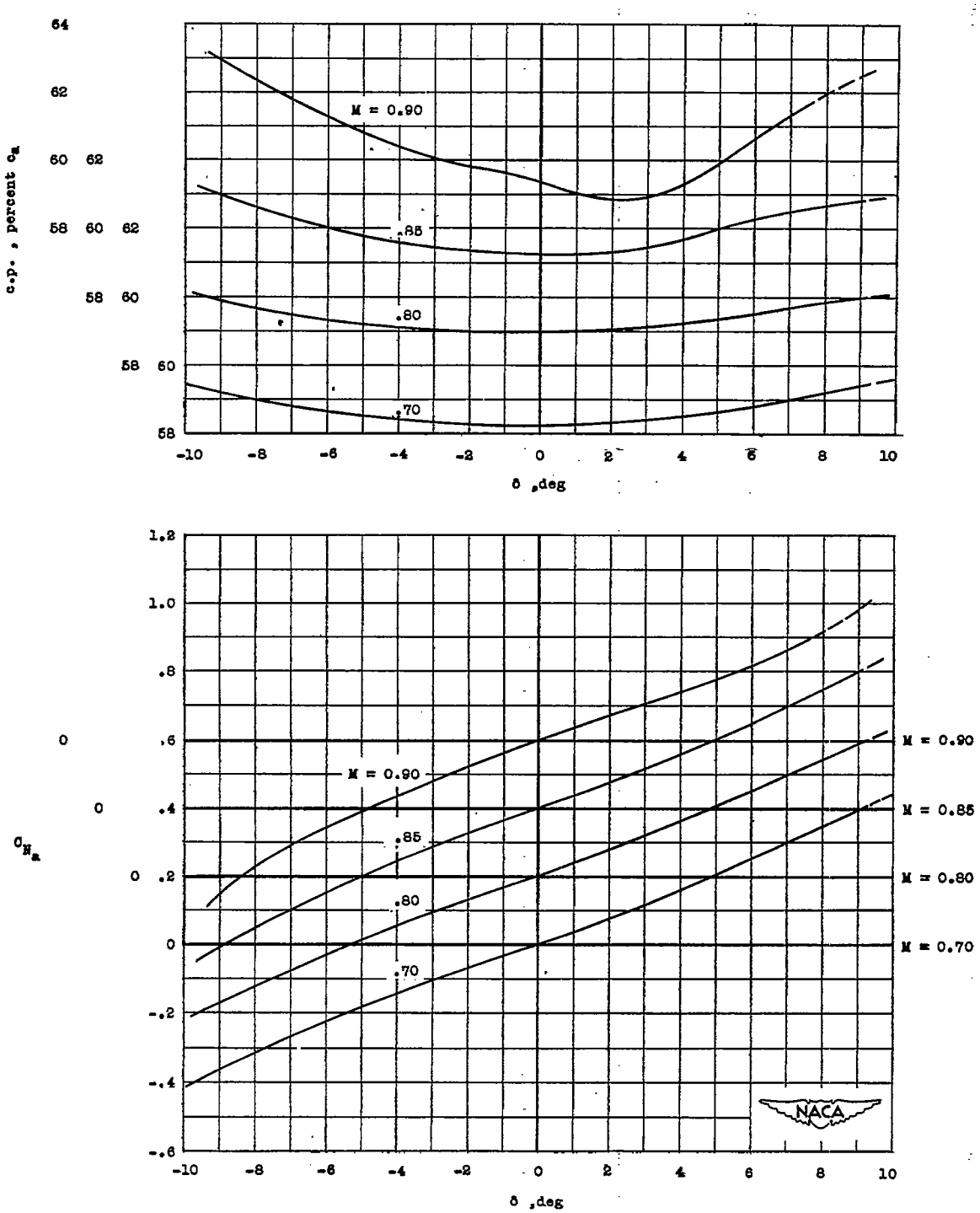

Figure 8.- Variation of control normal-force coefficient and chordwise center-of-pressure location with control deflection for M = 0.70 to M = 1.05, as determined by least squares application to the results of models A and B; $\alpha = 0^{\circ}$.

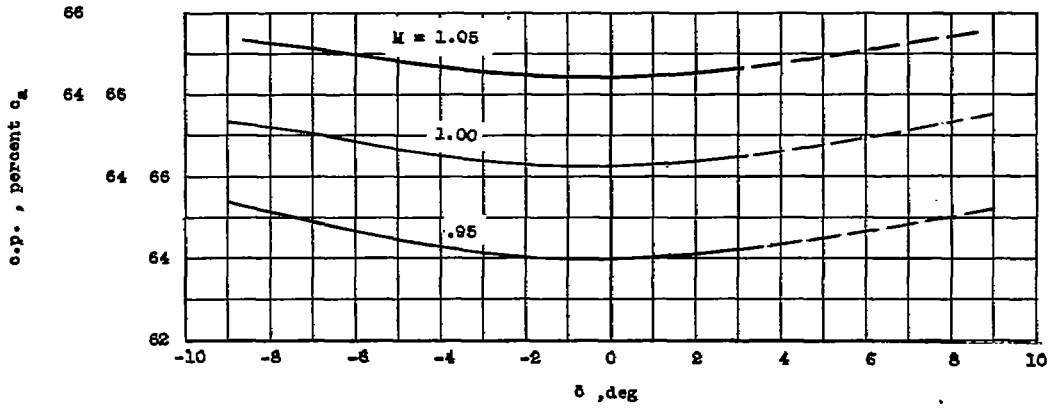

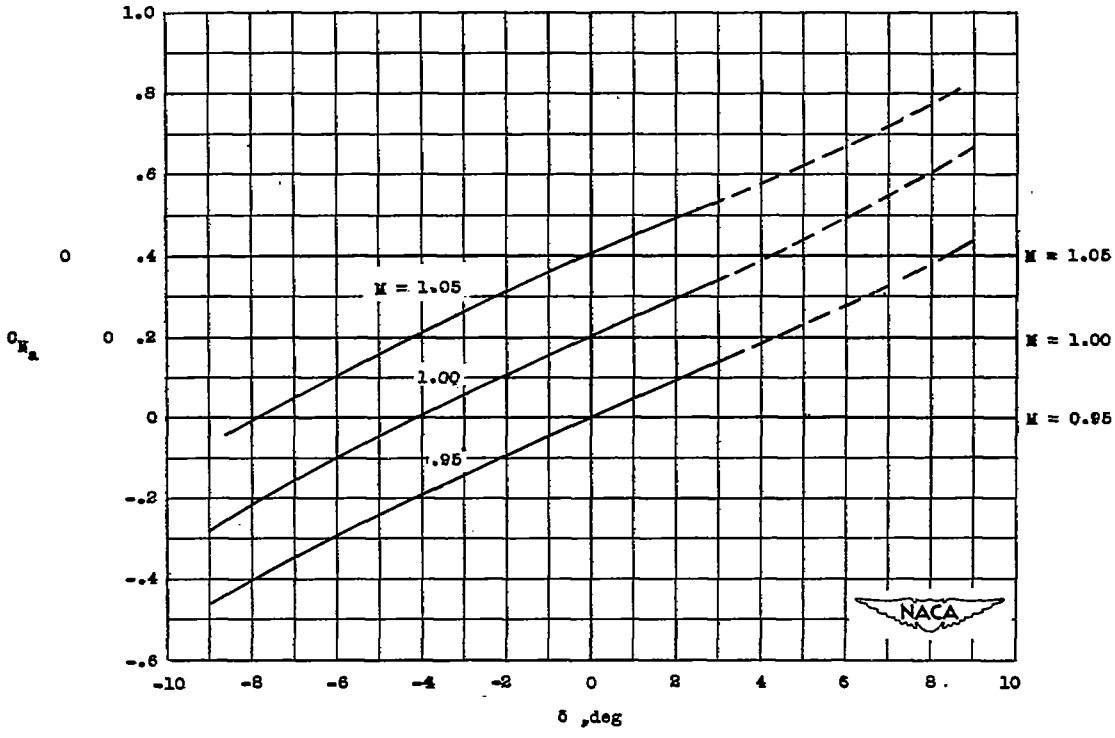

Figure 8.- Concluded.

[redacted]

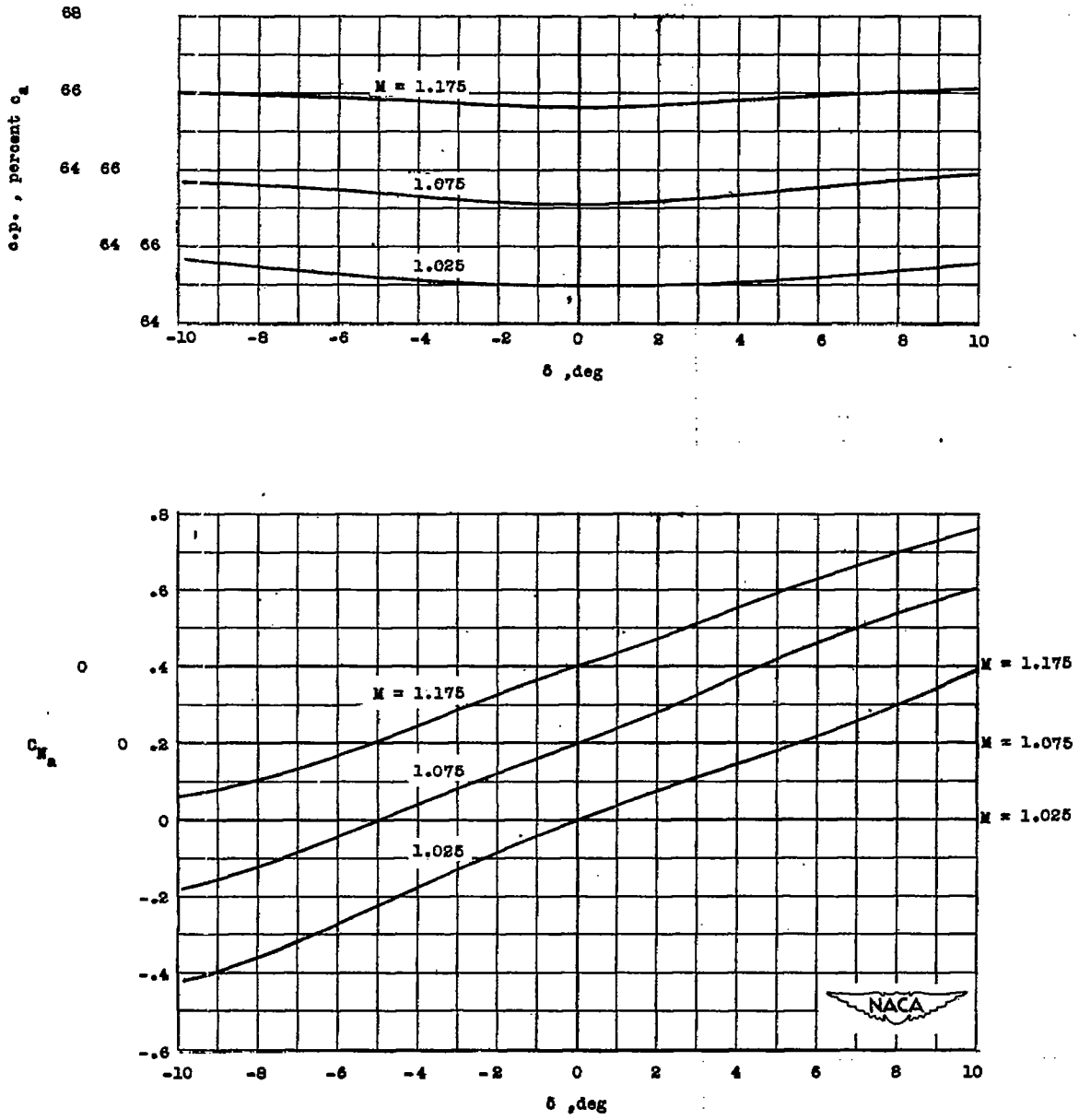

Figure 9.- Variation of control normal-force coefficient and chordwise center-of-pressure location with control deflection for $M = 1.025$ to $M = 1.435$ from model A results; $\alpha = 0^{\circ}$.

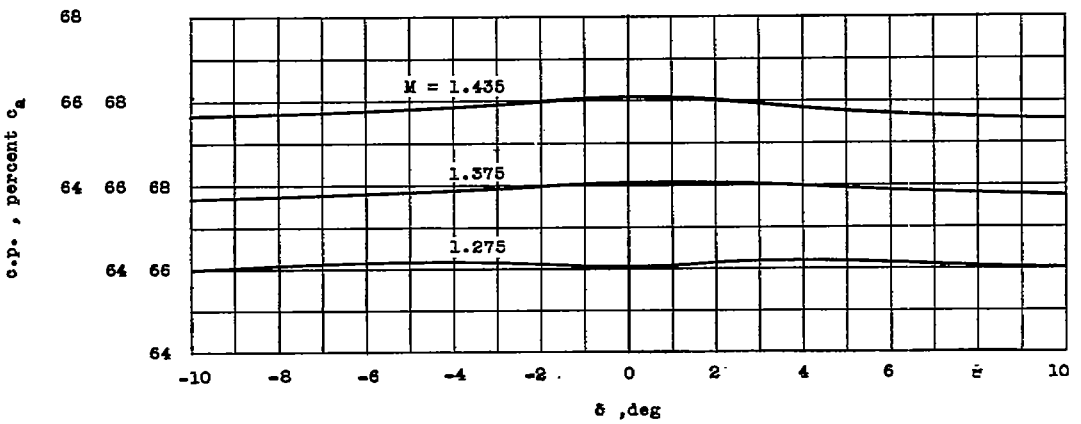

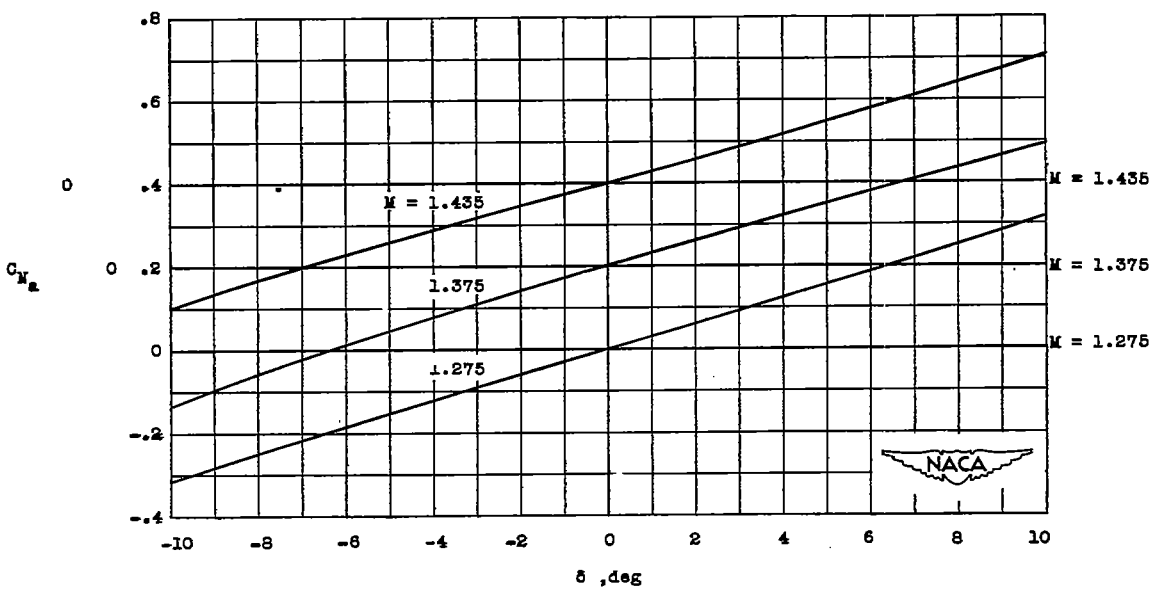

Figure 9.- Concluded.

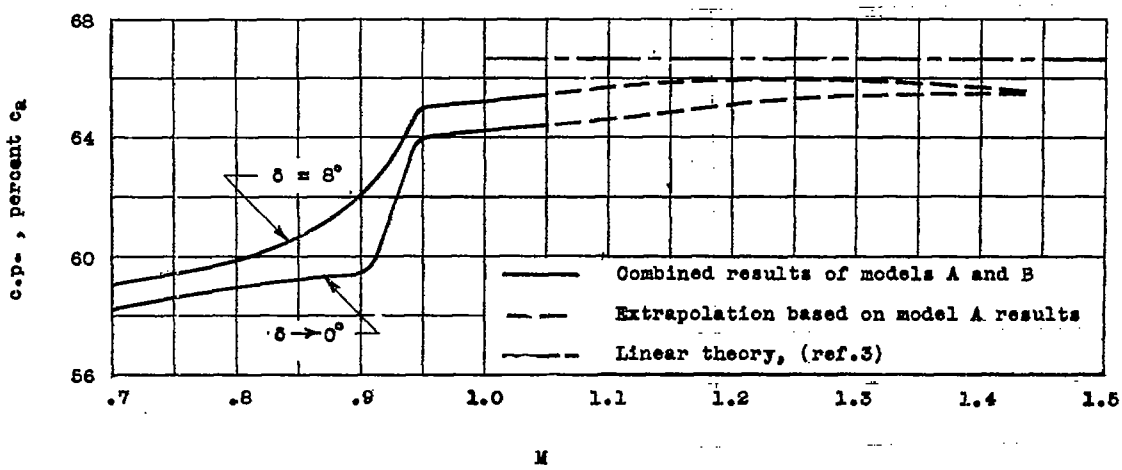

(a) Control chordwise center-of-pressure location.

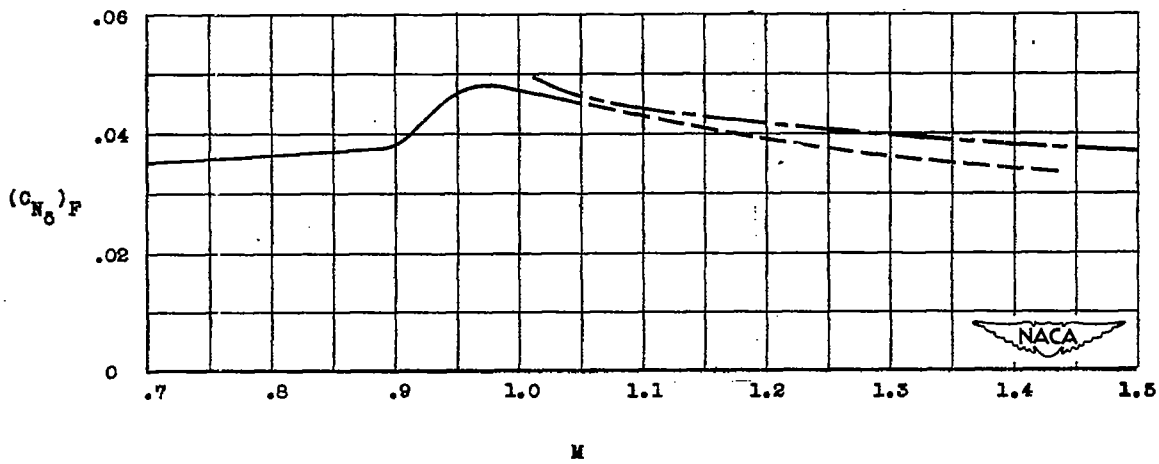

(b) Slope of the control normal-force-coefficient curve faired between $\delta = \pm 2^{\circ}$.

Figure 10.- Variation of faired control normal-force-coefficient slope and chordwise center-of-pressure location with Mach number.

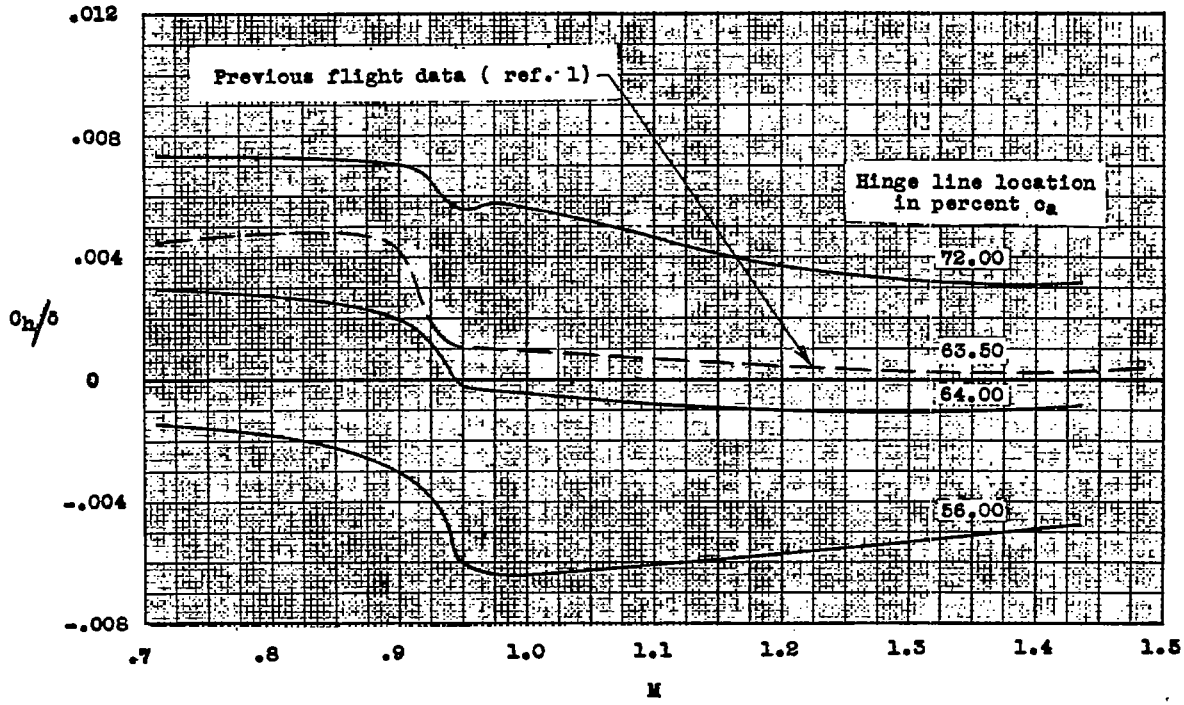

(a) Control hinge-moment coefficient per unit control deflection at $\delta = -5^{\circ}$.

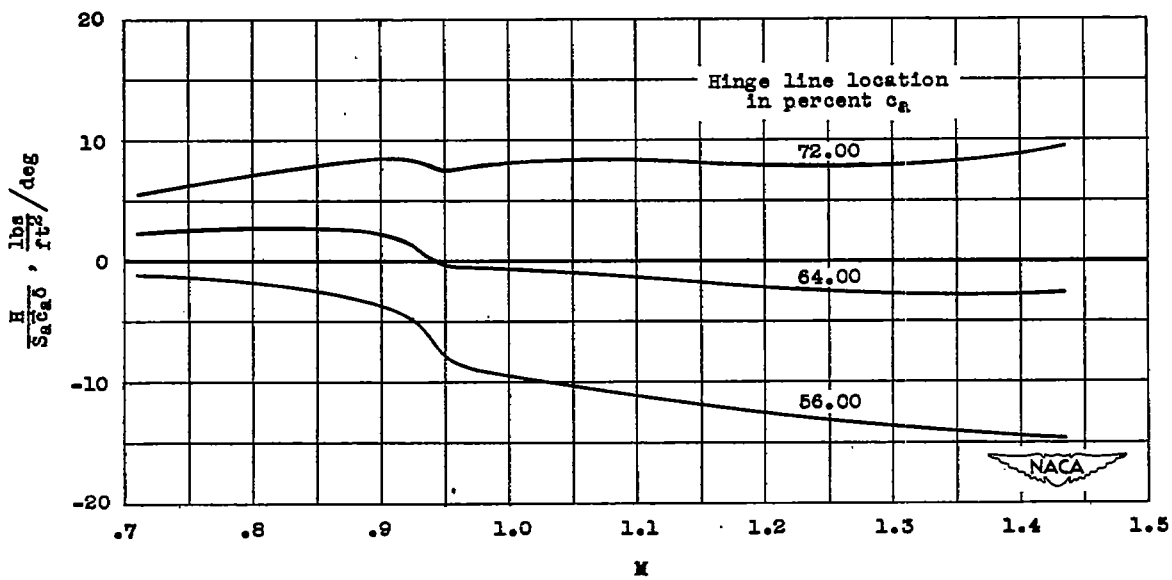

(b) Hinge-moment parameter $H/S_a\bar{c}_a\delta$ at $\delta = -5^{\circ}$.

Figure 11.- Control hinge-moment coefficient and parameter $H/S_a\bar{c}_a\delta$ against Mach number, as computed for various hinge-line locations.

[redacted]
SECURITY INFORMATION

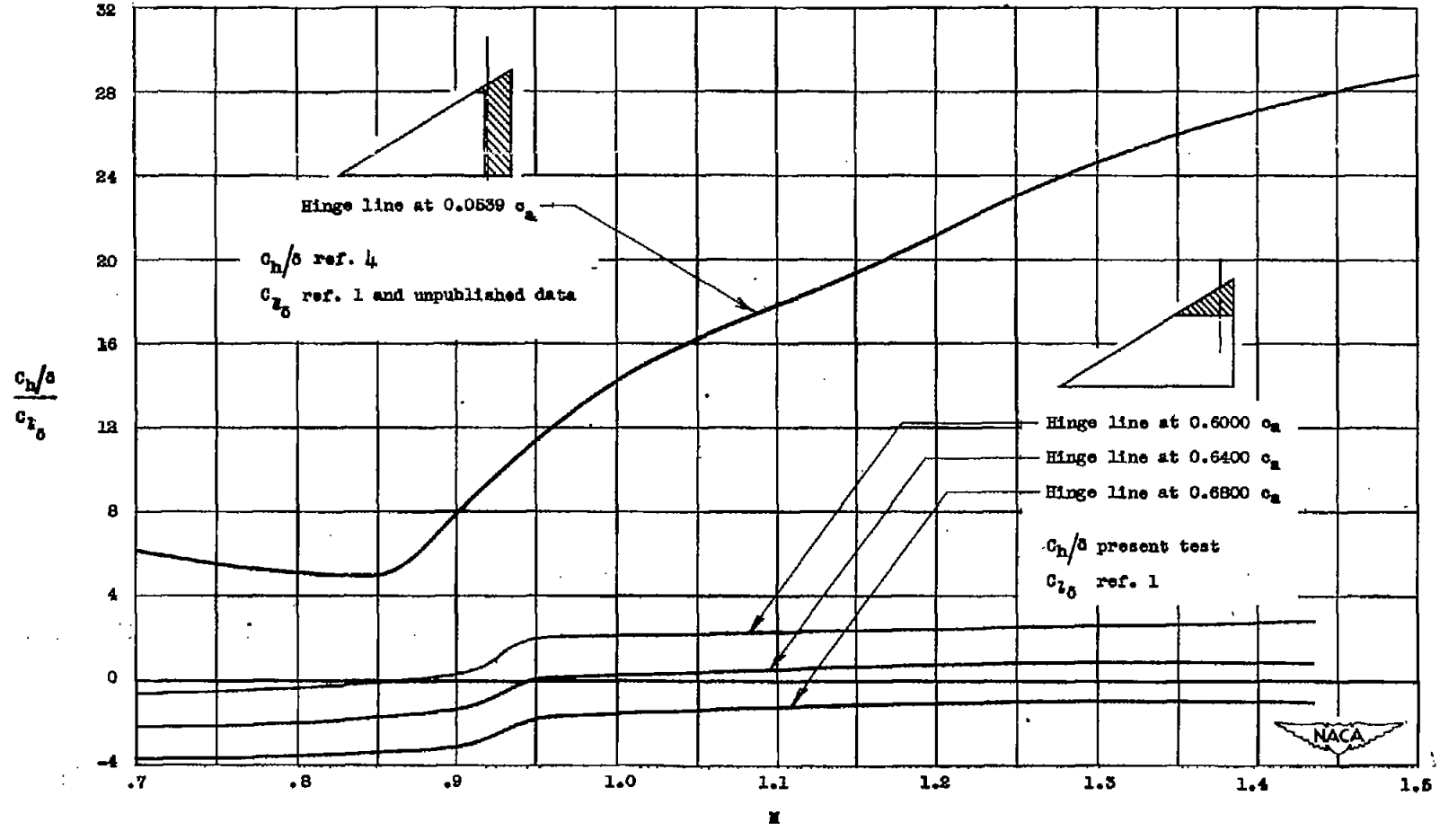

Figure 12.- Mach number variation of the control "effectiveness ratio" $\left(\frac{C_h/\delta}{C_{l_\delta}}\right)$ for a half-delta tip control (computed for three hinge line locations) and for a plain flap-type trailing-edge control; $\delta = -5^{\circ}$.

[redacted]
CONFIDENTIAL

NACA-Langley - 12-8-51 - 400